Science Bulletin 63 (2018) 419–425

Contents lists available at ScienceDirect

Science Bulletin

journal homepage: www.elsevier.com/locate/scib

Science Bulletin
www.scibull.com

Article

Epitaxially grown monolayer VSe_2: an air-stable magnetic two-dimensional material with low work function at edges

Zhong-Liu Liu [a,1], Xu Wu [a,1], Yan Shao [a,1], Jing Qi [a], Yun Cao [a], Li Huang [a], Chen Liu [b], Jia-Ou Wang [b], Qi Zheng [a], Zhi-Li Zhu [a], Kurash Ibrahim [b], Ye-Liang Wang [a,c,*], Hong-Jun Gao [a,c,*]

[a] Institute of Physics and University of Chinese Academy of Sciences, Chinese Academy of Sciences, Beijing 100190, China
[b] Institute of High Energy Physics, Chinese Academy of Sciences, Beijing 100049, China
[c] CAS Center for Excellence in Topological Quantum Computation, Beijing 100049, China

ARTICLE INFO

Article history:
Received 25 February 2018
Received in revised form 7 March 2018
Accepted 9 March 2018
Available online 20 March 2018

Keywords:
VSe_2
Two-dimensional materials
Magnetism
Epitaxial growth
Scanning tunneling microscopy (STM)

ABSTRACT

Recent experimental breakthroughs open up new opportunities for magnetism in few-atomic-layer two-dimensional (2D) materials, which makes fabrication of new magnetic 2D materials a fascinating issue. Here, we report the growth of monolayer VSe_2 by molecular beam epitaxy (MBE) method. Electronic properties measurements by scanning tunneling spectroscopy (STS) method revealed that the as-grown monolayer VSe_2 has magnetic characteristic peaks in its electronic density of states and a lower work-function at its edges. Moreover, air exposure experiments show air-stability of the monolayer VSe_2. This high-quality monolayer VSe_2, a very air-inert 2D material with magnetism and low edge work function, is promising for applications in developing next-generation low power-consumption, high efficiency spintronic devices and new electrocatalysts.

1. Introduction

Foreshadowed by early revelations of graphene's fantastic properties and potential applications, novel two-dimensional (2D) materials are attracting wide attention for both fundamental research [1–3] and application development [4–8], due to their unique structures and diverse properties [9]. Among 2D materials, magnetic 2D materials are quite intriguing due to their tremendous application prospects in low power-consumption, high efficiency spin-related computers and other nanoscale devices [10,11]. Theoretical works have predicted fantastic magnetic ordering in 2D materials, even in monolayers, in the past few years [12–16]. Very recently, magnetic properties have been observed experimentally in 2D CrI_3 and $Cr_2Ge_2Te_6$ materials [17–19]. These findings are stimulating fabrication of new magnetic 2D materials scaled down to the monolayer limit. Transition metal dichalcogenides (TMDC) are an emerging class of 2D materials with naturally layered structure. While applications of their electronic and optical functional properties have been very successful [20–23], investigation of their magnetic properties materials is still in its infancy, and hindered by a lack of both high-quality 2D samples and measurement techniques for magnetism in very thin samples. Vanadium diselenide (VSe_2) is a typical TMDC material with an MX_2 formula and a sandwiched layer structure. Both bulk phase [24] and multilayer film [25] have been reported to be ferromagnetic. Calculations predict the existence of magnetism even in monolayer VSe_2 [25–27]. As for the fabrication of VSe_2 materials, multilayer VSe_2 nanosheets 2.28–4.65 nm in thickness has been reported by mechanical exfoliation [25]. Multilayer VSe_2 nanosheets of various thicknesses from 4.9 to 90 nm have also been reported recently by CVD-grown method [28]. VSe_2 nanosheets containing small monolayer pieces around 80 nm in diameter have been obtained by chemical colloidal synthesis [29]. Currently, it is highly desirable to fabricate high quality monolayer VSe_2 and investigate its electronic properties for the development of this promising 2D material in novel electronic, spintronic or catalytic activities.

In this Article, we report growth of monolayer VSe_2 with unique properties on a highly oriented pyrolytic graphite (HOPG) substrate by molecular beam epitaxy (MBE). The selenium and vanadium atoms were deposited onto a cleaved and preheated HOPG surface, causing formation of a well-ordered monolayer structure, which was confirmed by scanning tunneling microscopy (STM). Then X-ray photoelectron spectroscopy (XPS) measurements were conducted to further confirm the chemical components and structure. Considering all the experimental observations together, we

* Corresponding authors.
E-mail addresses: ylwang@iphy.ac.cn (Y.-L. Wang), hjgao@iphy.ac.cn (H.-J. Gao).
[1] These authors contributed equally to this work.

https://doi.org/10.1016/j.scib.2018.03.008
2095-9273/

verified that the VSe_2 film fabricated on HOPG substrate is a 2D continuous monolayer. Besides homogenous morphology information, magnetism characteristic peaks were detected experimentally in the electronic density of states (DOS) through scanning tunneling spectroscopy (STS) measurements. Moreover, a sharp decline of local work function at the edge of the monolayer VSe_2 sheet was observed. Furthermore, the monolayer VSe_2 sheet was found to be quite inert in air. This high-quality epitaxial monolayer VSe_2 with air-stability, magnetism and low work function at its edge is promising for applications in spintronic devices and electrocatalysts.

2. Methods

2.1. Sample preparation

Monolayer VSe_2 was fabricated on an HOPG substrate in an ultrahigh vacuum (UHV) chamber, with a base pressure of 2×10^{-10} mbar, equipped with standard MBE capabilities. The HOPG substrate was cleaved and annealed to 1100 K in the UHV chamber. Selenium atoms (Sigma, 99.999%) were evaporated from a Knudsen cell, vanadium atoms (ESPI Metals, 99.999%) were evaporated from an electron-beam evaporator, and they were deposited onto the HOPG substrate, kept at 550 K. The growth parameters were under Se-rich conditions, with aiming to guarantee there are enough selenium atoms involving in reaction with vanadium. The excessive selenium atoms will be desorbed from the substrate since the substrate temperature at 550 K was higher than the evaporation temperature of selenium atoms (393 K). After growth, the samples were transferred to STM equipment and cooled for imaging and for measurement of the local electronic properties. In the air-exposure experiment, the samples were exposed to pure air for 24 h in a load-lock chamber and then transferred back into the UHV chamber to conduct STM and XPS measurements.

2.2. XPS measurements

The in situ X-ray photoelectron spectroscopy measurements were performed at the Beijing Synchrotron Radiation Facility (BSRF). Synchrotron radiation light monochromated by four high-resolution gratings and controlled by a hemispherical energy analyzer has photon energy in the range from 10 to 1,100 eV.

2.3. STM measurements

To obtain the topographies and electronic structures of the samples, STM experiments of the samples were performed at room temperature or a low temperature of 4.5 K. The differential conductance (dI/dV) was measured using lock-in detection of the tunnel current I by adding a 10 mV modulated bias voltage at 973 Hz to the sample bias voltage V. The feedback was switched off during the I-z measurements at a specific point, although it was kept on while the tip was moved on the sample.

3. Results and discussion

Fig. 1a is a schematic showing the fabrication procedure of monolayer VSe_2 film on the HOPG substrate through MBE. Selenium and vanadium atoms were deposited onto a HOPG substrate while it was heated at 550 K. The heated substrate provided the proper conditions for selenization of the vanadium atoms and formation of VSe_2 films as the vanadium atoms encountered excessive Se atoms. Unreacted Se atoms desorbed from the substrate since the substrate temperature (550 K) was much higher than

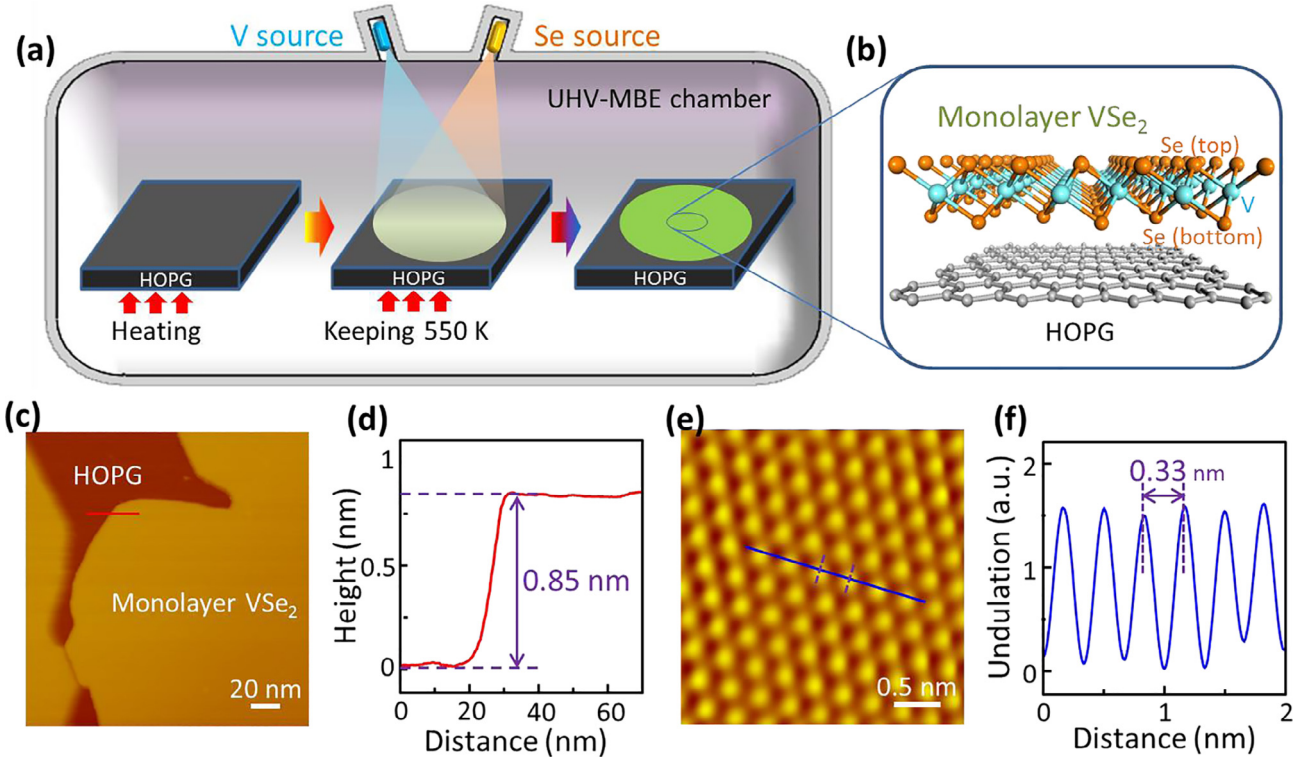

Fig. 1. (Color online) Monolayer VSe_2 formed on HOPG substrate. (a) Schematic of the fabrication process. (b) Structure schematic of VSe_2 on HOPG. (c) STM topographic image (−1.6 V, 0.1 nA) of VSe_2 on HOPG. (d) A height profile along the red line in (c), showing that the apparent height of VSe_2 is 0.85 nm. (e) Atomic resolution STM image (−1.3 V, 0.2 nA) of monolayer VSe_2 showing a hexagonal lattice. (f) Line profile corresponding to the blue line in (e), revealing the periodicity of the VSe_2 lattice (0.33 nm).

the evaporation temperature of Se atoms (393 K). The growth rate can be controlled by the vanadium flux since excess selenium atoms desorb from the substrate. And film coverage can be controlled by deposition time. An atomically smooth uniform film was obtained by optimization of these experimental parameters. As is shown by the schematic in Fig. 1b, monolayer VSe_2 contains one vanadium layer sandwiched between two Se layers are formed on the HOPG substrate.

In situ STM measurements were carried out at room temperature in order to gain a full understanding of the structural features of the VSe_2 film in detail. Fig. 1c shows a typical STM topographic image, revealing VSe_2 film on the HOPG surface, well ordered and very smooth. The apparent height of the VSe_2 film is ≈8.5 Å (Fig. 1d), as measured by the profile line across the edge of the VSe_2 film (corresponding to the red line in Fig. 1c). This apparent height is confirmed by atomic force microscope (AFM) measurements as shown in Fig. S1 (Online). Since the lattice constant in the *c* direction (the distance between two adjacent vanadium layers) is 6.105 Å in layered VSe_2 bulk [24], and considering the distance of the product with the substrate, the height of 8.5 Å is quite close to the thickness of monolayer VSe_2, and considerably smaller than that of bilayer VSe_2 (12.2 Å). This apparent height is in the value range of other monolayer TMDC materials on the substrates [30–33]. Thus the as-measured height provides direct evidence that the VSe_2 film formed on the HOPG surface has monolayer thickness.

An atomic-resolution STM image of monolayer VSe_2 is provided in Fig. 1e, in which a well-ordered hexagonal lattice can be clearly distinguished. The periodicity of this hexagonal lattice is revealed by the profile of the lattice, as depicted by the blue lines in Fig. 1f and e. This indicates a periodicity of 3.3 Å of the hexagonal lattice. This value of 3.3 Å matches well the Se-Se distance in the topmost Se sublayer, in accord with previous experimental results (3.356 Å) reported for bulk VSe_2 [24].

To confirm the chemical components and structure of the product, we conducted in situ XPS measurements. Characteristic peaks of both selenium and vanadium are found in the XPS spectra of as-grown VSe_2 film. Fig. 2a provides compares selenium 3d of the monolayer VSe_2 with that of selenium clusters (deposited on HOPG at room temperature). The binding energy positions of the selenium 3d peaks obviously differ between these two kinds of samples. The energy difference of 1.81 eV of these selenium 3d peaks indicates the change of chemical state from Se^0 (56.06 and 55.19 eV) to Se^{2-} (54.25 and 53.38 eV), which proves that selenium atoms in the film are chemically combined with the vanadium.

Fig. 2b and c provide a comparison of selenium 3d and vanadium 2p peaks of the monolayer VSe_2 with those of commercial bulk VSe_2, respectively. For the monolayer VSe_2, as shown in Fig. 2b, the characteristic signals of selenium $3d_{3/2}$ and $3d_{5/2}$ appear as peaks at their binding energies of 54.25 and 53.38 eV, respectively. And for bulk VSe_2, the binding energy positions of these two representative peaks are identical to those of monolayer VSe_2, and the shape of the curves are the same as well. Similarly, for the characteristic peaks ($2p_{1/2}$ and $2p_{3/2}$) of vanadium, as shown in Fig. 2c, there is also no obvious difference in either the binding energy positions or the shapes of the characteristic 2p peaks, between monolayer VSe_2 and bulk VSe_2. In short, comparison of XPS signals from both selenium and vanadium elements shows an accordance between bulk VSe_2 and as-grown monolayer VSe_2. This accordance in peaks suggests that the as-grown monolayer VSe_2 has the same 1T configuration with bulk VSe_2, since the 2H or 1T configuration of the TMDC materials can be distinguished by the element's characteristic peaks in XPS spectra [22,34,35], and the bulk VSe_2 exists naturally in 1T phase [24].

Magnetism was recently theoretically predicted [25] to exist in monolayer VSe_2 with a characteristic feature of two spin-reverse peaks in density of states (DOS) around the Fermi level. To further explore the magnetic properties of monolayer VSe_2, we carried out STS measurements at a low sample temperature of 4.5 K. Fig. 3a shows a STM topographic image of a monolayer VSe_2 island on the HOPG substrate. We measured d*I*/d*V* spectra both on the island and the substrate as marked by the purple (left) and black (right) points in Fig. 3a. The corresponding spectra are shown in Fig. 3b, revealing the local density of states (LDOS) of the sample. The LDOS curve of the substrate is in a peakless feature, indicating that the substrate has no effect to the electronic structure of VSe_2 monolayer.

As for the LDOS curve of the VSe_2 island, we can clearly distinguish two peaks around the theoretically predicted energy positions of the spin-reverse peaks [25], as marked by red (left) and blue (right) dashed lines in Fig. 3b, respectively. These peaks are fitted by Gauss function and reveal more precise energy positions at −0.28 and 0.23 eV, as shown in Fig. 3c and 3d. These energy values are in good agreement with the previous calculated ferromagnetism peaks of monolayer VSe_2 [25]. Hence, we believe that these observed peaks originate from intrinsic magnetism of the monolayer VSe_2. In addition, the curve shows a gap state between energy positions −0.08 and 0.08 eV, which can be ascribed to the state of charge density wave (CDW) of the monolayer VSe_2 at low sample temperature of 4.5 K (Fig. S2 online). This kind of excited state is

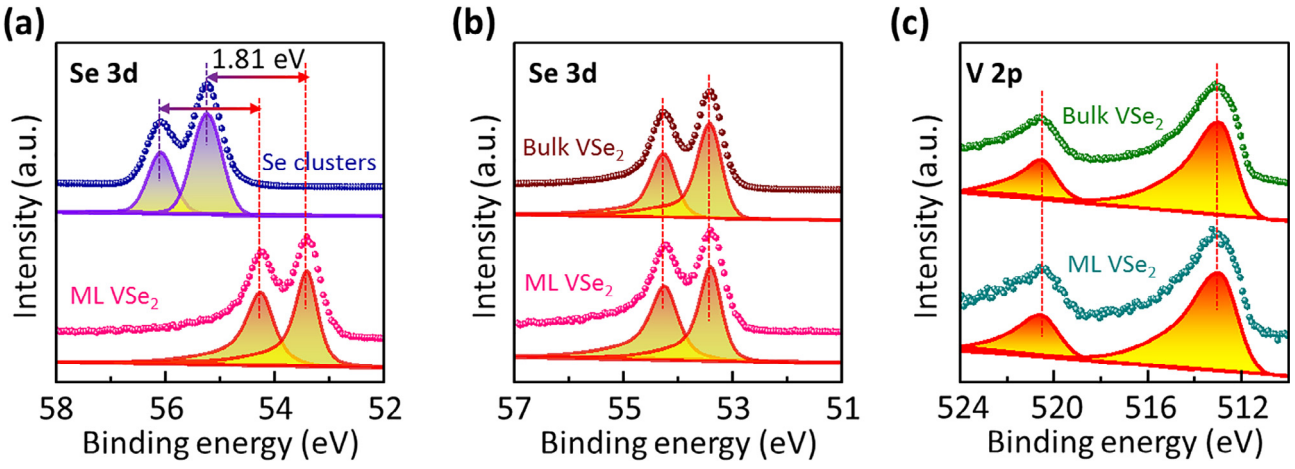

Fig. 2. (Color online) XPS results of Se clusters and VSe_2 samples. (a) The Se 3d spectra of the deposited Se clusters and monolayer VSe_2 on HOPG. The Se 3d peak positions (of Se clusters at 56.06 and 55.19 eV, of monolayer VSe_2 at 54.25 and 53.38 eV), showing an energy difference of 1.81 eV. (b) The Se 3d spectra of bulk VSe_2 and monolayer VSe_2. Peak positions at 54.25 and 53.38 eV are the same. (c) The V 2p spectra of bulk VSe_2 and monolayer VSe_2. Peak positions at 520.43 and 512.93 eV are the same.

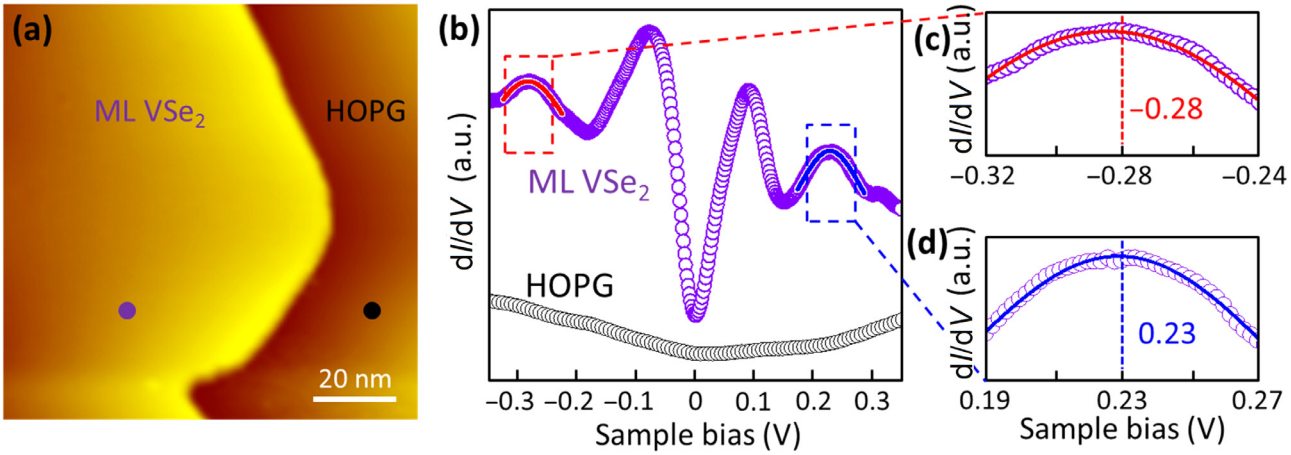

Fig. 3. (Color online) Electronic structures of monolayer VSe_2 on HOPG by STS measurements. (a) STM image of a monolayer VSe_2 island on the HOPG substrate. d*I*/d*V* spectra measured on the island and the substrate, showing by purple and black dots, respectively. (b) d*I*/d*V* spectra measured on the island and the substrate. Two peaks marked by red and blue lines correspond to the theoretically predicted spin-reverse peaks. (c) and (d) Gaussian-fitting of the two peaks marked in (b), the peak positions are −0.28 and 0.23 V, respectively.

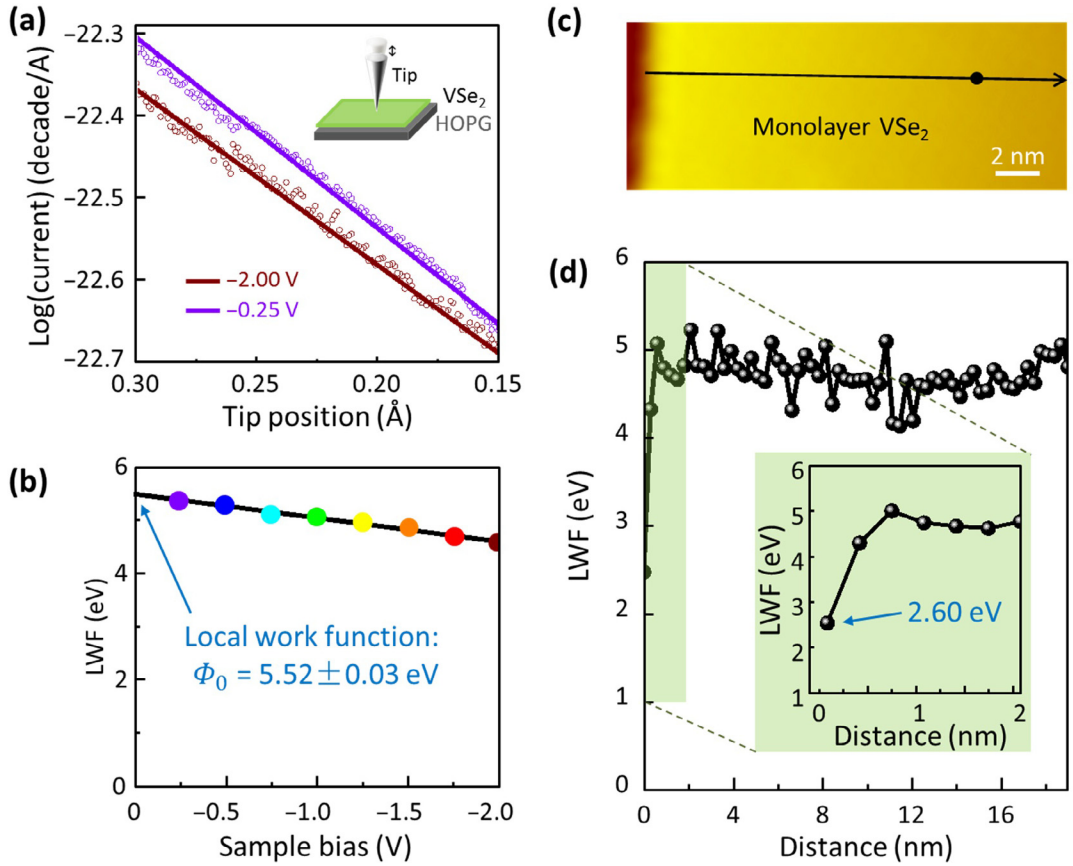

Fig. 4. (Color online) Local work-function (LWF) measurements of monolayer VSe_2. (a) *I*-*z* spectra obtained at the same location at the sample marked by the black point in (c) with different sample biases −2.00 and −0.25 V, described with logarithm in the vertical axis. Inset: Schematic of *I*-*z* spectrum measured at different tip-sample distances. (b) Linear-fitting of LWF measured at the same location with different sample biases. The intercept at zero bias of the fitting line represents the intrinsic LWF $\Phi_0 = 5.52 \pm 0.03$ eV. (c) Path depicted by a black arrow, along which the LWF was measured at different locations. (d) LWF measured along the arrow-line shown in (c). Inset: Zoom-in of the LWF profile of the closest five points to the edge of monolayer VSe_2, with a LWF of 2.60 eV at the edge.

often reported in the TMDC materials that exists at low temperature [36,37]. We further made a STS linear mapping (Fig. S3 online) which confirms the energy positions of ferromagnetism peaks are spatially uniform despite of the CDW state. In short, our STS experimental measurements match the previous theoretically prediction of a nontrivial magnetic property in monolayer VSe_2.

Combined STS measurements and theoretical calculations are often used to investigate the magnetism of 2D materials in past

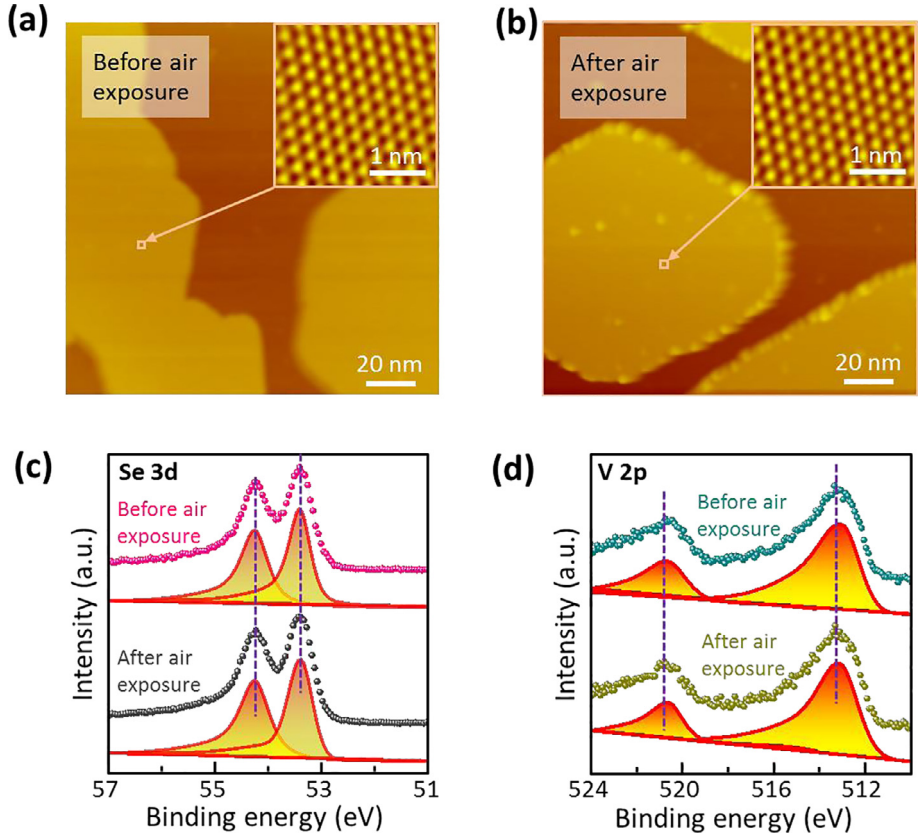

Fig. 5. (Color online) Air stability of monolayer VSe_2. (a) Typical STM image (−1.6 V, 0.1 nA) of monolayer VSe_2 on HOPG substrate before air exposure. The surface of the islands is smooth without impurities. Inset: Atomic resolution STM image (−1.3 V, 0.2 nA) of the monolayer VSe_2. (b) STM image (−1.6 V, 0.1 nA) of the sample after exposing to air. The surface of monolayer VSe_2 remains clean and smooth despite small adsorbates at the edge. Inset: Atomic resolution STM image (−1.3 V, 0.2 nA) of the lattice of monolayer VSe_2. (c) XPS measurements of the samples. The upper (pink), and lower (black) curves represent the Se 3d spectra before and after exposure to air, respectively. The peaks' positions (54.25 and 53.38 eV) and shapes in these curves do not change. (d) V 2p spectra before and after exposure to air. The peaks' positions (520.43 and 512.93 eV) and shapes in these curves also do not change.

years. For example, it is found practicable to detect the magnetism in hydrogen-adsorbed graphene and graphene nanoribbons [38,39]. Specifically, combined with ultrahigh-vacuum (UHV) and cryogenic conditions, STS can accomplish in-situ measurement of the as-grown sample in the same UHV system without sample transfer. This sample-transfer-free method holds advantage for preservation of the sample quality by avoiding possible contamination or adsorbates, very useful for the detection of the intrinsic properties like the relatively weak magnetism signal in 2D materials. In our current work, we also use in-situ STS technique to detect the possible magnetism signal of the as-grown VSe_2 sample. The STS curves show two characteristic peaks, an indication of magnetism, predicted in theoretical calculations. So we think that the STS measurements verify the theoretical calculations. Our STS measurements can be regarded as experimental evidence of the magnetism of monolayer VSe_2.

Besides the magnetic property, excellent electrocatalytic performance in hydrogen evolution reaction is reported for colloidal synthesized VSe_2 nanosheets [29]. In order to get a better understanding the mechanism of the electrocatalytic performance, we investigated the local work-function (LWF), which is often used to evaluate the electrocatalytic properties of materials. Fig. 4a presents two *I-z* curves obtained at the same point in monolayer VSe_2 film, marked in Fig. 4c, with different sample biases (−0.5 and −2.0 eV). It is obvious that the one with lower bias voltage has a steeper slope, showing that its LWF is higher. We measured more *I-z* curves with different sample biases from which we can get their corresponding LWFs. These LWFs, marked by color of their corresponding curves (for details see Fig. S4, online), were linear-fitted as shown in Fig. 4b. The intercept at zero bias of the fitting line represents the intrinsic work function of monolayer VSe_2 at this position: $\Phi_0 = 5.52 \pm 0.03$ eV, which is lower than the work function of bulk VSe_2, with its value of 5.76 eV [40].

Having assessed the intrinsic work function of monolayer VSe_2 film, we further investigated the LWF at the edge of the VSe_2 sheet by using the STM-based local probe technique. A linear mapping of LWF close to the edge of the VSe_2 sheet was measured along the black arrow as shown in Fig. 4c. Sixty-four points were measured in the mapping, as shown in Fig. 4d. We can see that LWF drops sharply at the edge, dramatically decreasing to 2.60 eV, almost half of the measured value in the rest of the film. Generally, a lower work function benefits electrocatalysis, since it reduces the energetic barrier for electrons to transfer from the electrocatalyst [41]. Thus, our spatially resolved measurements reveal a lower LWF value of monolayer and a plummet at the edge, which could explain the excellent electrocatalytic performance of the VSe_2 nanosheets [29].

Air-stability is critical for an atomic-thickness 2D material in practical applications. In order to evaluate the air-stability of monolayer VSe_2, air-exposure experiments of the samples were carried out. A sample with lower VSe_2 coverage, featuring small islands and plenty of island edges, was prepared for the experiment, since the chemical reactions of 2D materials normally start from the edges. For comparison, the sample was characterized by

STM and XPS before and after it was exposed to air and kept at room temperature for 24 h. Fig. 5a and b show STM images before and after air exposure. Although there were some adsorbates along the edges of islands after air exposure (Fig. 5b), the VSe_2 islands remained clean and smooth for the most part. The lattice structure of monolayer VSe_2 was completely preserved, as shown in the insets of Fig. 5a and b.

XPS measurements of selenium and vanadium characteristic peaks also show no obvious differences before and after air exposure, as shown in Fig. 5c. The pink curve (upper) and black (lower) curve, exhibiting Se $3d_{3/2}$ peak and Se $3d_{5/2}$ peak, are measured before and after air exposure, respectively. We can see that these two curves are consistent with each other in both peak positions and shapes. Similarly, in Fig. 5d, the curves of V $2p_{1/2}$ and $2p_{3/2}$ measured before (green curve online) and after (yellow curve online) air exposure are much alike. These combined measurements provide strong evidence that monolayer VSe_2 is quite inert to air. This air-stability is undoubtedly conducive to application of VSe_2 in related devices.

4. Summary

We report a facile and reliable growth method and structural characterization of high quality monolayer VSe_2, which is a prerequisite for any fundamental study and device applications. Electronic properties measurements by STS method revealed that the monolayer VSe_2 has magnetic characteristic peaks in its electronic density of states and a lower work-function at its edge. Moreover, air exposure experiments show the excellent stability of the monolayer VSe_2. This high-quality monolayer VSe_2, a very air-inert 2D material with magnetism and low work function at its edge, has promise for applications in developing next-generation spintronic devices and electrocatalyst-related devices.

Conflict of interest

The authors declare that they have no conflict of interest.

Acknowledgments

This work was supported by the National Natural Science Foundation of China (61725107, 51572290 and 11334006), National Key Research & Development Projects of China (2016YFA0202301), National Basic Research Program of China (2013CBA01601) and Strategic Priority Research Program (B) of Chinese Academy of Sciences (XDPB06).

Appendix A. Supplementary data

Supplementary data associated with this article can be found, in the online version, at https://doi.org/10.1016/j.scib.2018.03.008.

References

[1] Bandurin DA, Torre I, Kumar RK, et al. Negative local resistance caused by viscous electron backflow in graphene. Science 2016;351:1055–8.
[2] Li LF, Lu SZ, Pan JB, et al. Buckled germanene formation on Pt(111). Adv Mater 2014;26:4820.
[3] Wu X, Shao Y, Liu H, et al. Epitaxial growth and air-stability of monolayer antimonene on $PdTe_2$. Adv Mater 2017;29:1605407.
[4] Wang YQ, Wu X, Wang YL, et al. Spontaneous formation of a superconductor-topological insulator-normal metal layered heterostructure. Adv Mater 2016;28:5013–7.
[5] Miller OD, Ilic O, Christensen T, et al. Limits to the optical response of graphene and two-dimensional materials. Nano Lett 2017;17:5408–15.
[6] Chhowalla M, Shin HS, Eda G, et al. The chemistry of two-dimensional layered transition metal dichalcogenide nanosheets. Nat Chem 2013;5:263–75.
[7] Wang YL, Li LF, Yao W, et al. Monolayer $PtSe_2$, a new semiconducting transition-metal-dichalcogenide, epitaxially grown by direct selenization of Pt. Nano Lett 2015;15:4013–8.
[8] Zhang SL, Guo SY, Chen ZF, et al. Recent progress in 2D group-VA semiconductors: from theory to experiment. Chem Soc Rev 2018;47:982–1021.
[9] Tan CL, Cao XH, Wu XJ, et al. Recent advances in ultrathin two-dimensional nanomaterials. Chem Rev 2017;117:6225–331.
[10] Soumyanarayanan A, Reyren N, Fert A, et al. Emergent phenomena induced by spin-orbit coupling at surfaces and interfaces. Nature 2016;539:509–17.
[11] Han W, Kawakami RK, Gmitra M, et al. Graphene spintronics. Nat Nanotechnol 2014;9:794–807.
[12] Sun LL, Zhou W, Liu YY, et al. A first-principles study on the origin of magnetism induced by intrinsic defects in monolayer SnS_2. Comp Mater Sci 2017;126:52–8.
[13] Manchanda P, Skomski R. 2D transition-metal diselenides: phase segregation, electronic structure, and magnetism. J Phys Condens Matter 2016;28:064002.
[14] Lebegue S, Bjorkman T, Klintenberg M, et al. Two-dimensional materials from data filtering and Ab Initio calculations. Phys Rev X 2013;3:031002.
[15] Kulish VV, Huang W. Single-layer metal halides MX_2 (X= Cl, Br, I): stability and tunable magnetism from first principles and Monte Carlo simulations. J Mater Chem C 2017;5:8734.
[16] Kan M, Wang B, Lee YH, et al. A density functional theory study of the tunable structure, magnetism and metal-insulator phase transition in VS_2 monolayers induced by in-plane biaxial strain. Nano Res 2015;8:1348–56.
[17] McGuire MA, Dixit H, Cooper VR, et al. Coupling of crystal structure and magnetism in the layered, ferromagnetic insulator CrI_3. Chem Mater 2015;27:612–20.
[18] Huang B, Clark G, Navarro-Moratalla E, et al. Layer-dependent ferromagnetism in a van der Waals crystal down to the monolayer limit. Nature 2017;546:270–3.
[19] Gong C, Li L, Li Z, et al. Discovery of intrinsic ferromagnetism in two-dimensional van der Waals crystals. Nature 2017;546:265–9.
[20] Wang QH, Kalantar-Zadeh K, Kis A, et al. Electronics and optoelectronics of two-dimensional transition metal dichalcogenides. Nat Nanotechnol 2012;7:699–712.
[21] Ross JS, Rivera P, Schaibley J, et al. Interlayer exciton optoelectronics in a 2D heterostructure p-n junction. Nano Lett 2017;17:638–43.
[22] Lin X, Lu JC, Shao Y, et al. Intrinsically patterned two-dimensional materials for selective adsorption of molecules and nanoclusters. Nat Mater 2017;16:717.
[23] Bhimanapati GR, Lin Z, Meunier V, et al. Recent advances in two-dimensional materials beyond graphene. ACS Nano 2015;9:11509–39.
[24] Bayard M, Sienko M. Anomalous electrical and magnetic properties of vanadium diselenide. J Solid State Chem 1976;19:325–9.
[25] Xu K, Chen P, Li X, et al. Ultrathin nanosheets of vanadium diselenide: a metallic two-dimensional material with ferromagnetic charge-density-wave behavior. Angew Chem Int Ed 2013;52:10477–81.
[26] Ma Y, Dai Y, Guo M, et al. Evidence of the existence of magnetism in pristine VX_2 monolayers (X= S, Se) and their strain-induced tunable magnetic properties. ACS Nano 2012;6:1695–701.
[27] Liu J, Hou WJ, Cheng C, et al. Intrinsic valley polarization of magnetic VSe_2 monolayers. J Phys Condens Matter 2017;29:255501.
[28] Zhang Z, Niu J, Yang P, et al. Van der Waals epitaxial growth of 2D metallic vanadium diselenide single crystals and their extra-high electrical conductivity. Adv Mater 2017;1702359.
[29] Zhao W, Dong B, Guo Z, et al. Colloidal synthesis of VSe_2 single-layer nanosheets as novel electrocatalysts for the hydrogen evolution reaction. Chem Commun (Camb) 2016;52:9228–31.
[30] Zhao Y, Qiao J, Yu P, et al. Extraordinarily strong interlayer interaction in 2D layered PtS_2. Adv Mater 2016;28:2399–407.
[31] Wang XL, Gong YJ, Shi G, et al. Chemical vapor deposition growth of crystalline mono layer $MoSe_2$. ACS Nano 2014;8:5125–31.
[32] Zhang Y, Zhang YF, Ji QQ, et al. Controlled growth of high-quality monolayer WS_2 layers on sapphire and imaging its grain boundary. ACS Nano 2013;7:8963–71.
[33] Li H, Zhang Q, Yap CCR, et al. From bulk to monolayer MoS_2: evolution of raman scattering. Adv Funct Mater 2012;22:1385–90.
[34] Voiry D, Mohite A, Chhowalla M. Phase engineering of transition metal dichalcogenides. Chem Soc Rev 2015;44:2702–12.
[35] Qu Y, Medina H, Wang SW, et al. Wafer scale phase-engineered 1T-and 2H-$MoSe_2$/Mo Core–shell 3D-hierarchical nanostructures toward efficient electrocatalytic hydrogen evolution reaction. Adv Mater 2016;28:9831–8.
[36] Zhang D, Ha J, Baek H, et al. Strain engineering a $4a\times\sqrt{3}a$ charge-density-wave phase in transition-metal dichalcogenide 1T-VSe_2. Phys Rev Mater 2017;1:024005.
[37] Ugeda MM, Bradley AJ, Zhang Y, et al. Characterization of collective ground states in single-layer $NbSe_2$. Nat Phys 2015;12:92–7.
[38] Gonzalez-Herrero H, Gomez-Rodriguez JM, Mallet P, et al. Atomic-scale control of graphene magnetism by using hydrogen atoms. Science 2016;352:437–41.
[39] Magda GZ, Jin XZ, Hagymasi I, et al. Room-temperature magnetic order on zigzag edges of narrow graphene nanoribbons. Nature 2014;514:608.
[40] Claessen R, Schafer I, Skibowski M. The unoccupied electronic structure of 1T-VSe_2. J Phys Condens Matter 1990;2:10045.

[41] Cheon JY, Kim JH, Kim JH, et al. Intrinsic relationship between enhanced oxygen reduction reaction activity and nanoscale work function of doped carbons. J Am Chem Soc 2014;136:8875–8.

Zhong-Liu Liu received his B.S. degree from University of Science and Technology of China in 2014. He is now studying at Institute of Physics (IOP), Chinese Academy of Sciences (CAS) for his Ph.D. degree. His current research interest focuses on the two-dimensional functional materials.

Yeliang Wang received his B.S. and M.S. degree from the Wuhan University of Technology, Ph.D. degree from IOP, CAS. He then joined in the Max-Planck-Institute for Solid Research, Germany as a Humboldt Fellow. He was appointed an associate professor in 2008 and a full professor in 2013 in the IOP, CAS. He was awarded as The National Science Fund for Distinguished Young Scholars in 2017. His current research interest is the epitaxial fabrication and properties of novel two-dimensional materials.

Hong-jun Gao received his Ph.D. degree in physics from Peking University in 1994. He then joined in the Nanoscale Physics and Devices Laboratory of IOP, CAS. Now, he is an Academician of the CAS and an Academician of the Developing-Country Academy of Sciences. His research interest is the construction and physical property of low-dimensional nanostructures, and scanning tunneling microscopy/spectroscopy.